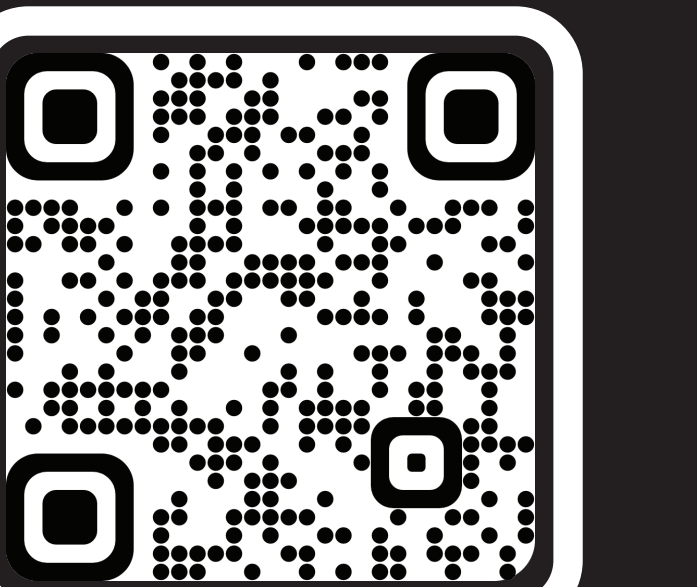


Bottom Boundary Layer Dynamics In the Iceland Scotland Overflow Along The Reykjanes Ridge

Manish S. Devana, William E. Johns

University of Miami, Rosenstiel School of Marine and Atmospheric Science

Contact: devanamarsci@gmail.com



Please Scan for
further analysis
and contact
info

1 Introduction

The Iceland Scotland Overflow is a deep ocean current in the North Atlantic that is a key component of the Atlantic Meridional Overturning Circulation. The current is formed from Nordic Sea deep waters overflowing across the Iceland Faroe Ridge into the abyssal layers of the Iceland Basin and entraining mid-depth Atlantic Waters along the descent. The flow goes on to be a topographically steered current following the Iceland Basin westward towards the Reykjanes Ridge where it turns south and is eventually exported into various regions of the North Atlantic.

The Overturning in the Subpolar North Atlantic Program (OSNAP) mooring array monitors the ISOW flow as it is exported from the Iceland Basin. The bottom intensified flow moves along the rugged topography of the Reykjanes Ridge's eastern flank. The interactions with this topography are expected to force non linear flow responses and generated bottom intensified mixing. These processes range from mesoscale down to small scale but may have cumulative effects that leave imprints on the large scale ISOW flow and water mass properties.

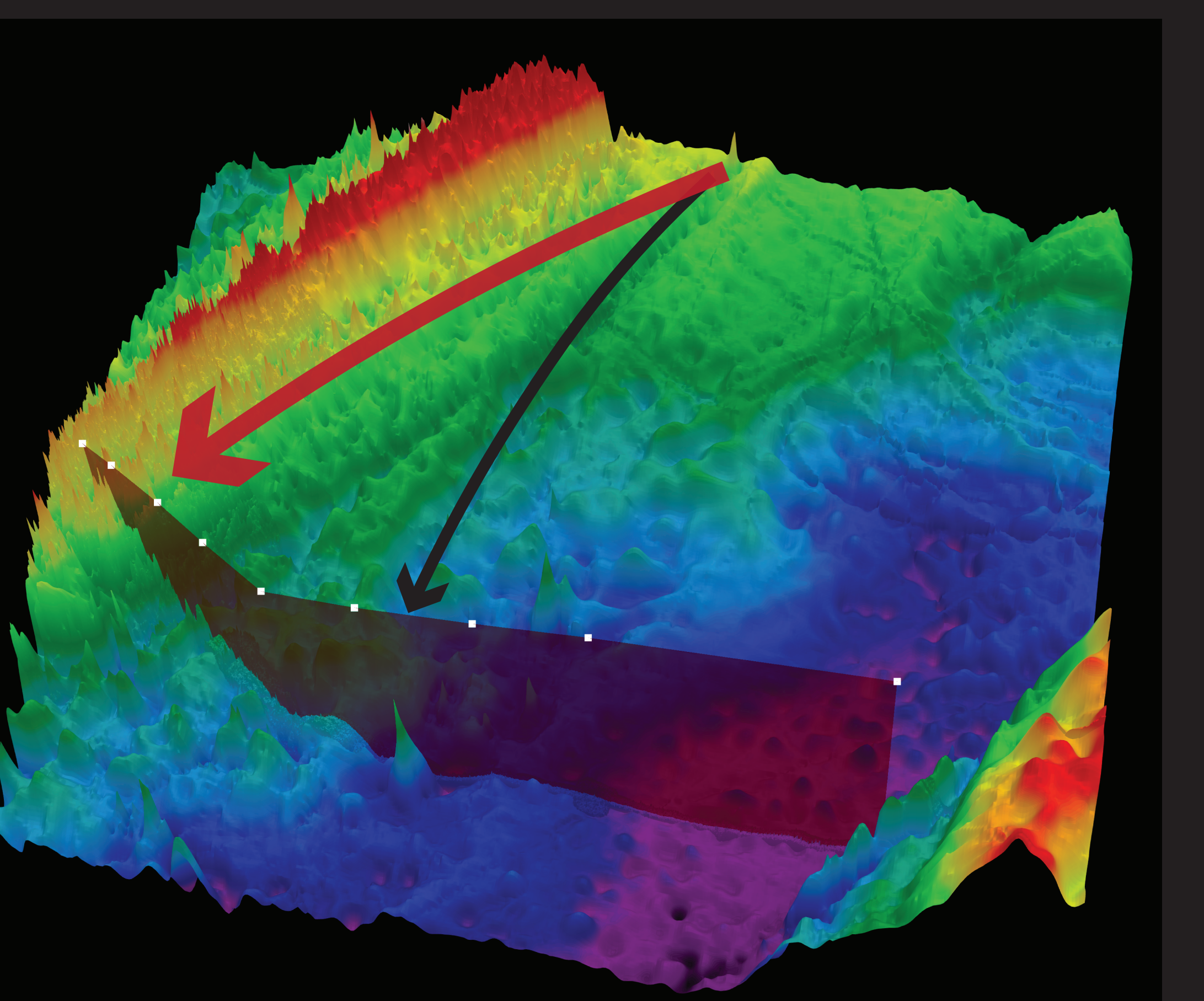


Figure 1: GEBCO bathymetry of the Iceland Basin with OSNAP mooring locations indicated. Arrows depict mean flow pathways of ISOW. Shaded red slice shows OSNAP mooring section with mooring locations indicated at white squares. Arrows indicate 2 mean flow pathways. This work is focused largely on the red pathway

2 Motivation

Mooring observations and repeat hydrographic sections show a thick (2-300 meter) bottom boundary layer typically located near the top of the ridge flank (Fig 2). Interior isopyncals deflect upwards before plunging downwards into the topography. This structure is observed in the mean from mooring observations (white isopyncal, Fig. 2) and hydrographic sections. Isopyncal structure during periods of elevated boundary layer thickness are similar to the mean state (orange isopyncal, Fig. 2) while periods of reduced boundary layer thickness show notably more flat isopyncal structure (blue isopyncal, Fig. 2).

A range of studies have highlighted the particular importance of boundary layers on sloping bottoms which can contain intense small scale mixing¹, submesoscale instabilities^{2,6,7}, drive exchanges between the boundary layer and interior ocean^{3,6}, and impart large scale abyssal overturning⁴. OSNAP observations have also shown a progressive expansion of the ISOW layer as it moves along the ridge. It has been theorized that this may be linked to small scale dynamics in the flow

This work aims first identify the dynamics governing the mean state large boundary layer, examine the mechanisms that erode the layer, and finally determine the impacts of these processes on the ISOW as it is exported into the lower layers of the North Atlantic.

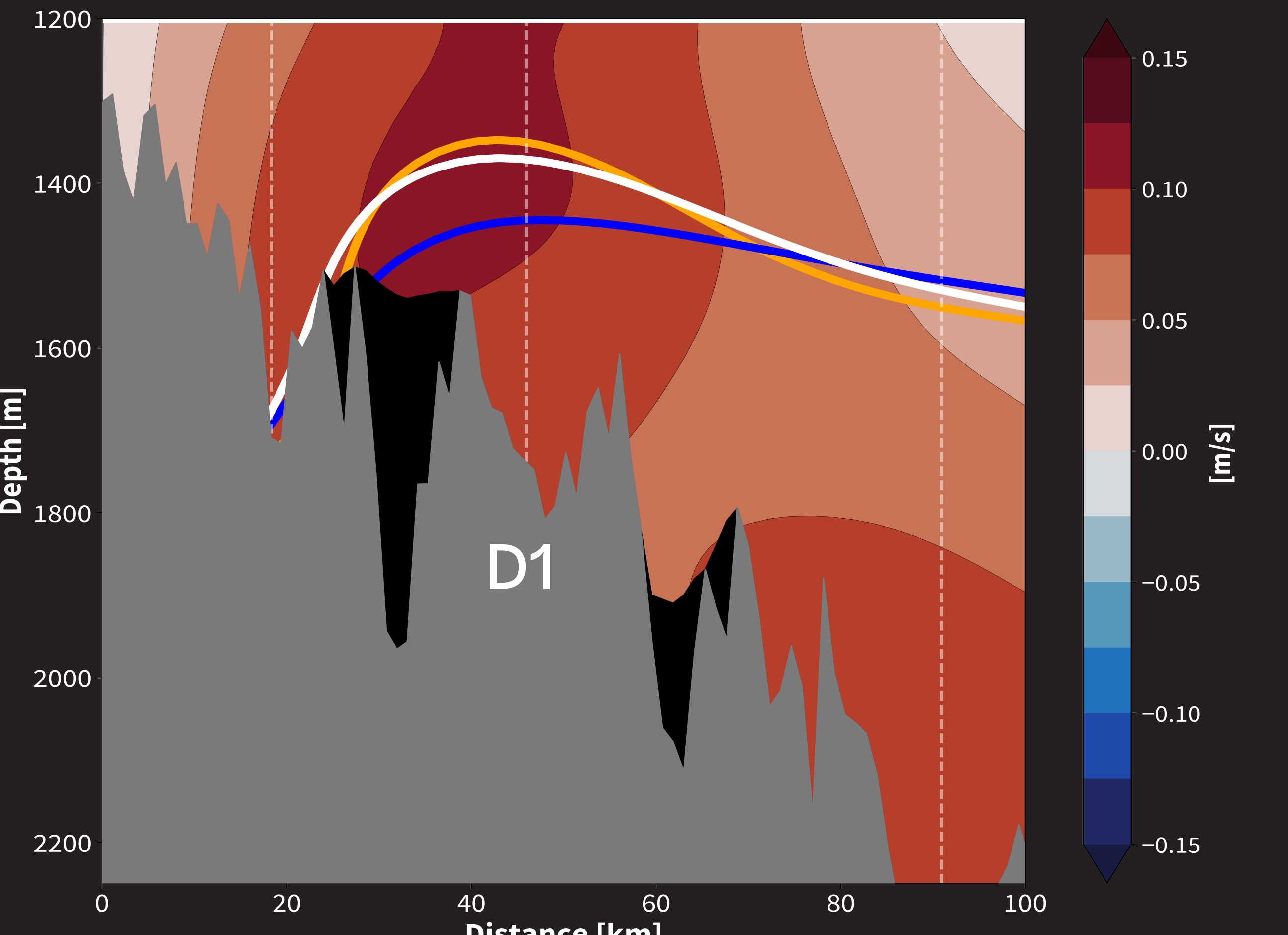


Figure 2: Mean along slope flow at section of OSNAP array near the Reykjanes Ridge crest. Values are positive southwards out of the Iceland Basin. 27.8 isopycnal (the upper boundary of ISOW) is shown for the mean (white), high (orange) and low (blue) boundary layer thickness. D1 mooring is indicated as the remaining analyses presented here is focused on this mooring.

3 Boundary Layers Along Slopes

Flow along insulating sloping bottom boundaries can generate cross slope flows through the frictional bottom Ekman layer that arises from the bottom friction⁵. In the case of ISOW the Ekman flow is downslope and leads to a downslope buoyancy advection and a buoyancy gradient normal to the slope. However, since no flux is permitted through the boundary, the isopyncals plunge downwards to remove the slope normal gradient in a layer extending further into the interior than the frictional layer. This layer grows until the shear is strong enough to bring the bottom flow to zero, a process known as Ekman Arrest⁵.

Bottom intensified mixing is also likely occur in these layers which leads upward doming of isopyncals before plunging downwards. Mixing and cross slope ekman flows can work in concert to grow the mixing layer to be several hundreds of meters thick⁴. The total combined boundary layer can then drive both cross slope and boundary to interior exchanges.

We suspect a combination of turbulent mixing and Ekman arrest dynamics to be acting on the ISOW layer. However we should note that these dynamics are complicated by the corrugated bottom topography and the near inertial flow variability^{3,6}.

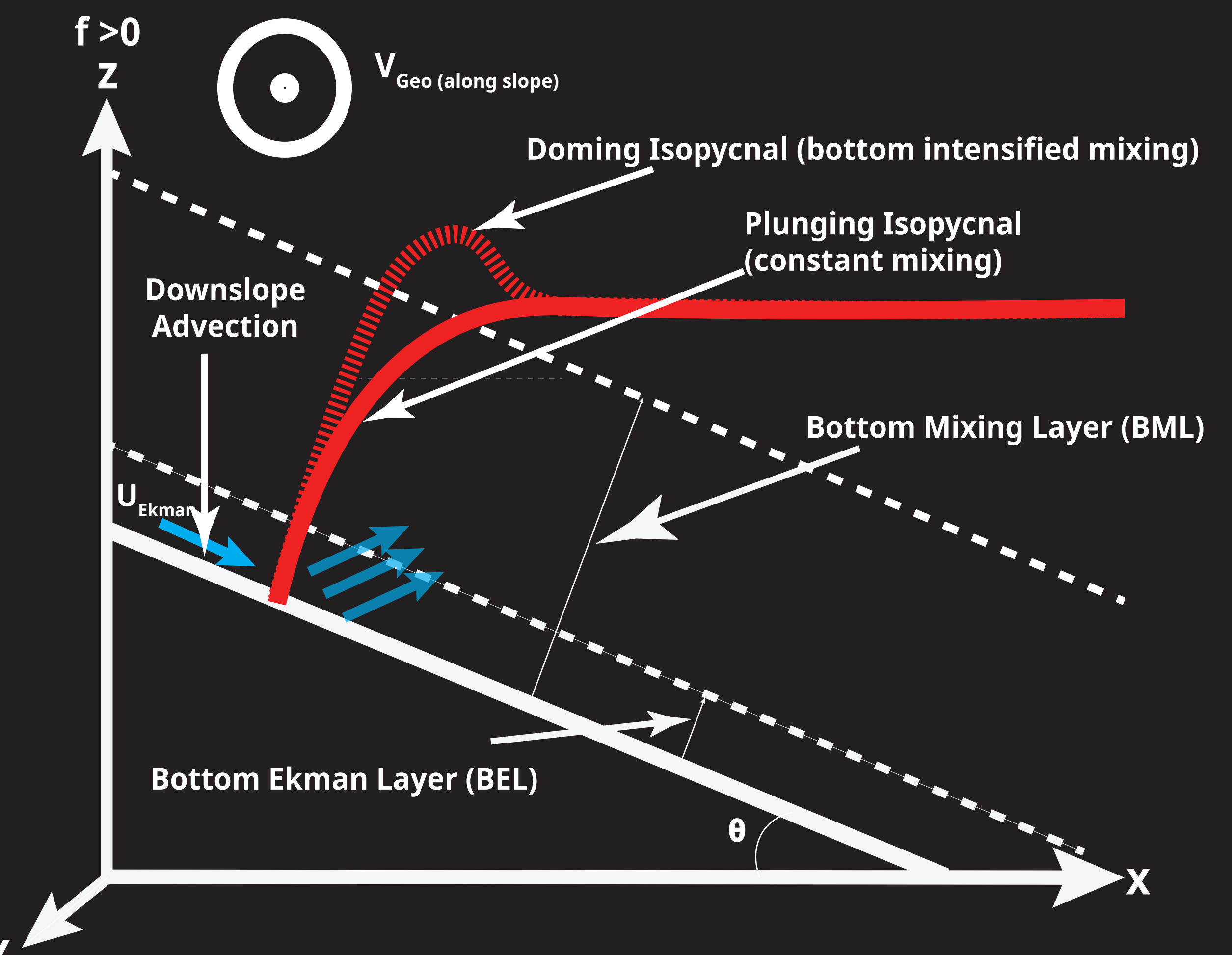


Figure 3: Schematic of processes along sloping bottom summarizing key processes described by Garrett et al. (1993). Isopyncals are shown in red and dashed lines indicate bottom Ekman and bottom mixing layer thicknesses. The total bottom boundary layer is taken as the upper bound of the mixing layer.

4 Mean Flow & Turbulent Diffusivity

The mean vertical diffusivity profile is estimated by applying the Thorpe Scales method to repeat OSNAP CTD profiles at the D1 mooring (Fig 2). The results show bottom intensification of mixing and the profile shape agrees well with a simple exponential profile in the form $K_0 + K_1 e^{(z/h)}$, where K_0 and K_1 are the interior and bottom diffusivity, respectively, and h is the vertical decay scale.

The mean flow shows strong along slope flow that weakens with depth while the cross slope flow increases in the down slope direction until 1500m. This indicates that the mean flow is veering down slope in the bottom ~200 meters, as one might expect in a large bottom mixing layer.

The values of diffusivity both at the bottom and the interior are higher than the estimates along the Mid Atlantic Ridge in the Brazil Basin (St. Laurent et. al. 2001). However, given the rough topography and vigorous ISOW flow, these elevated mixing rates are likely reasonable estimates.

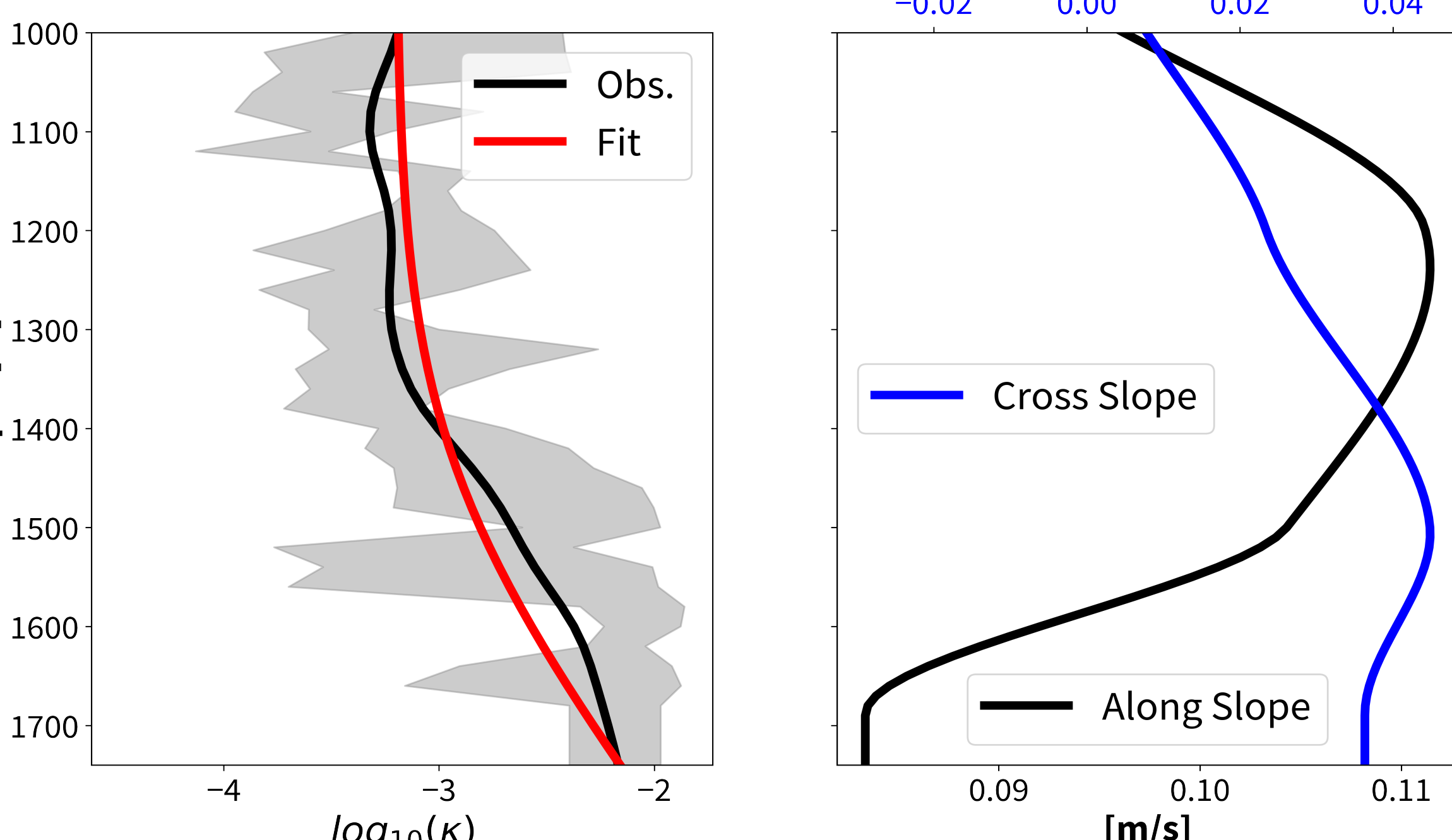


Figure 4: (left) Turbulent diffusivity estimated from repeat CTD sections using Thorpe Scales. Vertical low passed filter of mean observational k profile (black) and fit to exponential form (red) with parameters: (l) Gray shading indicates \pm std. deviation. (right) Mean along (black) and cross (blue) slope Pchip spline profile from moored current meters. Note that different scales are chosen to better compare the vertical structure.

5 Boundary Layer Evolution

The bottom boundary layer frequently collapses for 2-3 days. To analyze the observations in the periods of collapse we generate a 20 day composites of the data centered around the minimum in boundary layer thickness. The composites are the average of all collapse events over the 6 years of mooring observations.

Boundary layer collapses are typically preceded by a weakening of the along slope flow and oscillations in the cross slope flow. During the minimum or flat state of the boundary layer, downslope flow is weak and occasionally reverses.

The growth of the boundary layer after collapse appears to be driven by resurgence of the along slope flow as would be expected for the generation of an arrested Ekman layer.

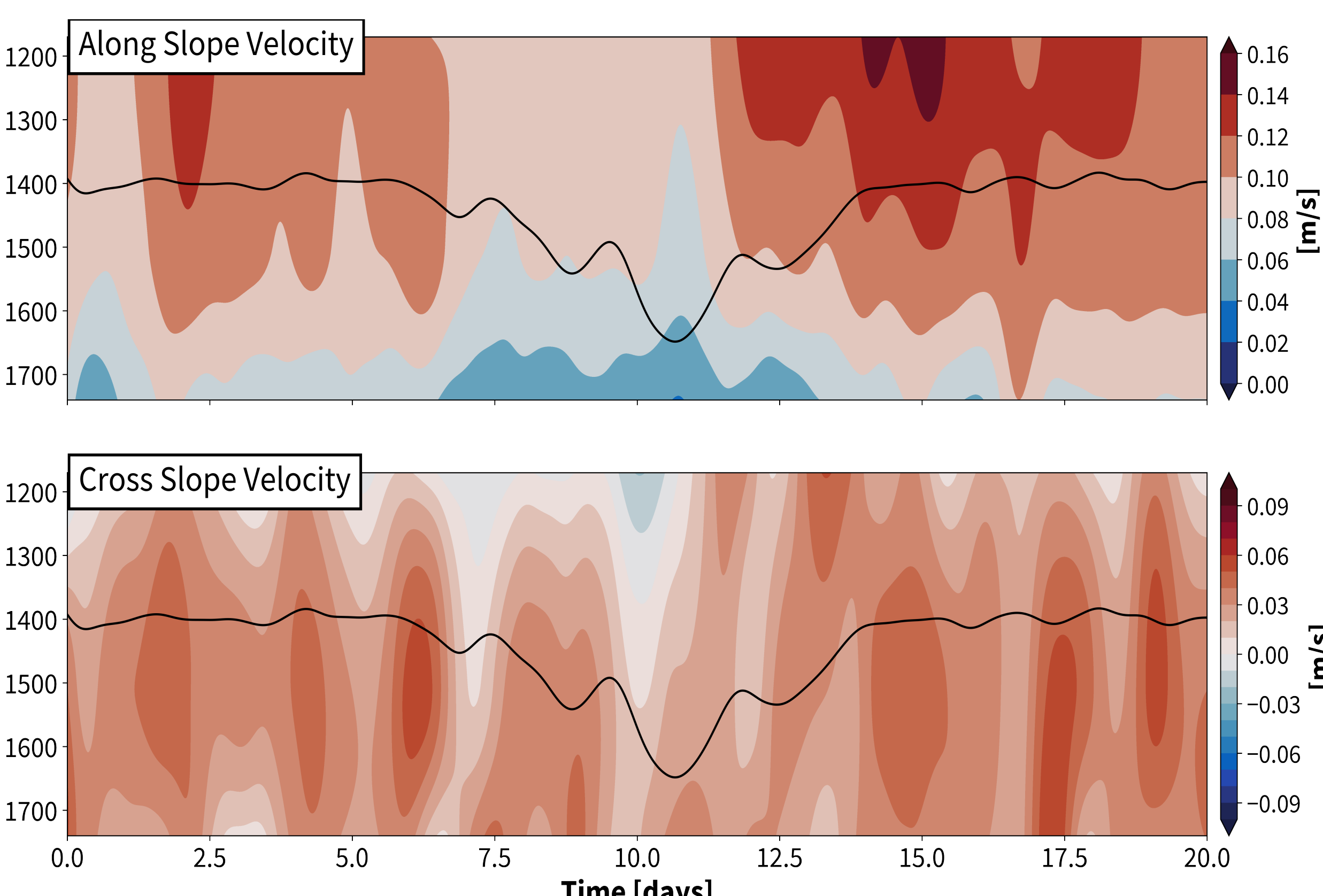


Figure 5: 20 day composite of the along (top) and cross (bottom) slope velocities at the D1 mooring. Composites are generated by averaging all 20 day periods centered on boundary layer collapses. Black line shows the composite mixed layer depth evolution. A 3 day low-pass filter is applied.

6 Internal Tides

The composite analysis above was extended to examine wavelets of the eddy kinetic energy during the periods of boundary layer collapse. Notable peaks in EKE occur at the M2 tidal frequency during the collapse of the boundary layer.

The M2 frequency bursts of EKE occur for 3-5 day periods but do not appear to occur at any regular intervals. This suggests that these short increases in tidal energy are unlikely to be linked to the spring-neap cycle. Instead these irregular bursts point to both internal tide generation and breaking of remotely generated internal tides.

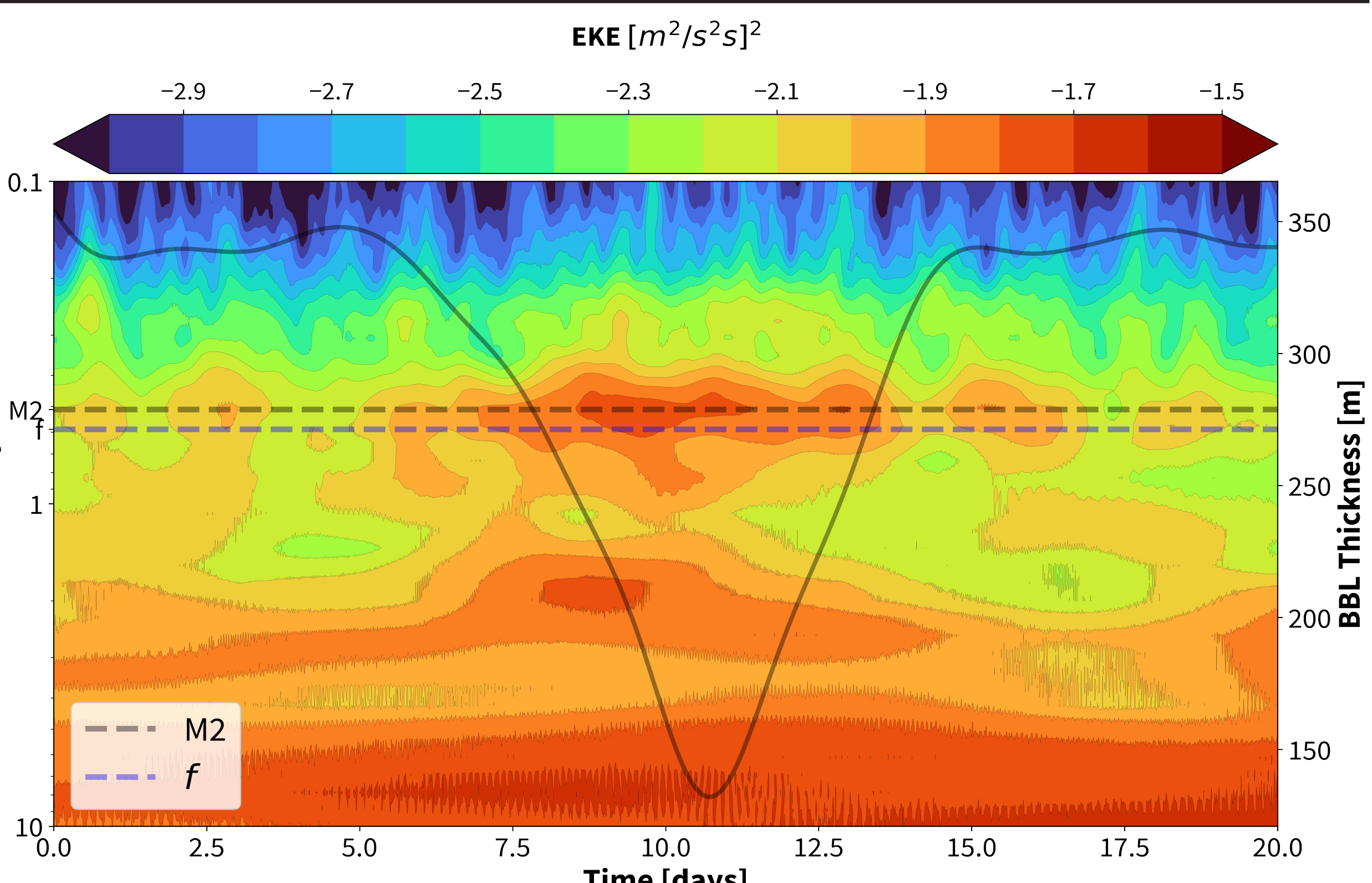


Figure 6: 20 day composite of eddy kinetic energy wavelet at the bottom current meter (1690m) at D1. Composite is centered around boundary layer collapse as in Figure 5. Dashed lines indicate the inertial and M2 periods. Solid black line shows the 3 day low passed composite of boundary layer thickness.

7 Key Findings

1. The large bottom boundary layer in ISOW flow shows clear bottom enhanced mixing and downslope veering of flow through the mixing layer.
2. Boundary layer collapses coincide with weakening along slope flow and strong fluctuations in cross slope flow.
3. Wavelet analysis displays M2 tidal peaks of eddy kinetic energy during collapse events. These bursts of tidal frequency energies suggests the presence of internal tides along the ridge flank.

8 Future Work

1. Develop method for quantifying exchanges with interior layers and across the slope.
2. Assess the role of corrugated bottom topography on the development of boundary layer
3. Explore role of PV in bottom boundary layer towards generation of instabilities.
4. Growth and collapse of boundary layer combined with intense mixing may be facilitate significant watermass transformations within ISOW and with adjacent water masses.

References

1. Brink, K. H., & Lentz, S. J. (2010). Buoyancy Arrest and Bottom Ekman Transport. Part I: Steady Flow. *Journal of Physical Oceanography*, 40(4), 621–635. <https://doi.org/10.1175/2009JPO4266.1>
2. Callies, J. (2018). Restratiification of Abyssal Mixing Layers by Submesoscale Baroclinic Eddies. *Journal of Physical Oceanography*, 48(9), 1995–2010. <https://doi.org/10.1175/JPO-D-18-0082.1>
3. Dell, R. W., & Pratt, L. J. (2015). Diffusive boundary layers over varying topography. *Journal of Fluid Mechanics*, 769, 635–653. <https://doi.org/10.1017/jfm.2015.88>
4. Drake, H. F., Ferrari, R., & Callies, J. (2020). Abyssal Circulation Driven by Near-Boundary Mixing: Water Mass Transformations and Interior Stratification. *Journal of Physical Oceanography*, 50(8), 2203–2226. <https://doi.org/10.1175/JPO-D-19-0313.1>
5. Garrett, C., MacCready, P., & Rhines, P. (1993). Boundary Mixing and Arrested Ekman Layers: Rotating Stratified Flow Near a Sloping Boundary. *Annual Review of Fluid Mechanics*, 25(1), 291–323. <https://doi.org/10.1146/annurev.fl.25.010193.001451>
6. Ruan, X., & Thompson, A. F. (2016). Bottom Boundary Potential Vorticity Injection from an Oscillating Flow: A PV Pump. *Journal of Physical Oceanography*, 46(11), 3509–3526. <https://doi.org/10.1175/JPO-D-15-0222.1>
7. Wenegrat, J. O., Callies, J., & Thomas, L. N. (2018). Submesoscale Baroclinic Instability in the Bottom Boundary Layer. *Journal of Physical Oceanography*, 48(11), 2571–2592. <https://doi.org/10.1175/JPO-D-17-0264.1>